PROCEEDINGS OF SCIENCE

QCD Results from LHCb

Giovanni Passaleva[*†]
Istituto Nazionale di Fisica Nucleare (INFN) - Florence
E-mail: giovanni.passaleva@fi.infn.it

The LHCb experiment, besides its main programme of b and c-physics, also performs very well as a general purpose forward detector, covering the pseudo-rapidity range 2.0 to 5.0. Exploiting the experiment's unique geometry, the LHCb collaboration is pursuing a rich programme of forward QCD measurements. A selection of these results will be presented, highlighting the capabilities of LHCb as a general purpose experiment.

Fourth Annual Large Hadron Collider Physics
13-18 June 2016
Lund, Sweden

[*]Speaker.
[†]On behalf of the LHCb collaboration

PoS(LHCP2016)135

1. Introduction

The LHCb experiment [1] was designed for CP violation measurements and rare decays involving b and c-hadrons at the LHC. It consists of a single arm spectrometer fully instrumented with tracking, calorimetry and particle identification in the pseudorapidity range $2 < \eta < 5$. The silicon strip vertex detector that surrounds the interaction point provides further coverage in the backward region, in the approximate range $-3.5 < \eta < -1.5$. This unique coverage of the forward region, together with excellent tracking and particle identification performances, allows probing of particle production at the LHC in an uncharted region of phase space. The pseudorapidity coverage has been further improved for the $\sqrt{s} = 13$ TeV run with the installation of forward shower counters [2], consisting of five planes of scintillators perpendicular to the beam at about ± 114 m, ± 20 m and -7.5 m from the interaction point. With the additional counters LHCb has sensitivity to particles in the regions $-10 < \eta < -5$, $-3.5 < \eta < -1.5$, $1.5 < \eta < 10$. In addition, LHCb is designed to trigger on particles produced at low transverse momentum and runs at a reduced instantaneous luminosity in low pile–up conditions. All these features make LHCb well suited for QCD studies especially in the forward region, complementary to other LHC experiments. LHCb has published already a large number of measurements related to QCD studies including jet production in association with vector bosons, vector boson and top quark production, hadron production cross–sections, soft QCD studies and, more recently, heavy ion physics. In these proceedings, results on central exclusive production (CEP) of heavy quarkonia and on multi parton interactions are summarised. The measurements discussed in the following are obtained from data collected by LHCb at $\sqrt{s} = 7$ TeV and $\sqrt{s} = 8$ TeV, with an integrated luminosity of about 1 fb^{-1} and 2 fb^{-1} respectively.

2. Central exclusive production of heavy quarkonia

Central exclusive production (CEP) at LHC consists of a diffractive process that at the leading order (LO) proceeds through the exchange of two photons, two pomerons, or a photon and a pomeron between the two intact colliding protons. The events are characterised by an isolated system of particles surrounded by two rapidity gaps with respect to the diffractive protons [3, 4]. At LHC, photon-photon and photon-pomeron fusion probe the photon and the gluon content of the proton at parton fractional momenta, x, directly comparable with past electron-ion colliders; at central rapidities x values of the order of 10^{-4} are probed, similar to those examined at HERA. However, at the forward rapidities accessible to the LHCb experiment, the x reach extends to 5×10^{-6}. The measurements performed at LHCb are based on detection of final states with muons. In particular, photoproduction of single and double charmonia, and single bottomonium has been studied [5–7].

2.1 Photoproduction of J/ψ and $\psi(2S)$ mesons

Candidates for J/ψ ($\psi(2S)$) mesons produced through CEP are selected by requiring two identified muons inside the pseudorapidity range $2 < \eta(\mu^{\pm}) < 4.5$ and no photons or additional tracks in either forward or backward directions [5]. The dimuon invariant mass is required to be within 65 MeV/c^2 of the known J/ψ or $\psi(2S)$ masses. To enhance the diffractive component of the signal, the p_T^2 of the reconstructed candidate mesons must be smaller than 0.8 GeV^2/c^2. The

invariant mass of all candidates is shown in Fig. 1 (left). The non–resonant background is modelled with an exponential function and represents (0.8±0.1)% of the J/ψ and (16±3)% of the $\psi(2S)$ sample. Feed-down backgrounds inside the J/ψ mass window, due to radiative decays of χ_c and $\psi(2S)$ where the photon goes undetected, is estimated from simulation, normalised to data using $\chi_c \to J/\psi\gamma$ and $\psi(2S) \to J/\psi\pi\pi$ candidates and amounts to (10.1±0.9)%. Inelastic charmonium production, in which the proton dissociates outside the LHCb acceptance, is estimated by fitting the $t \simeq p_T^2$ distribution and assuming that $d\sigma/dt$ can be modelled by two exponentials for signal and background, as predicted by Regge theory and observed at HERA [6, 7]. The fit is performed on the J/ψ ($\psi(2S)$) p_T^2 distribution, after subtracting the non–resonant background estimated from the invariant mass distribution sidebands as shown in Fig. 1. The fitted parameters for the exponentials

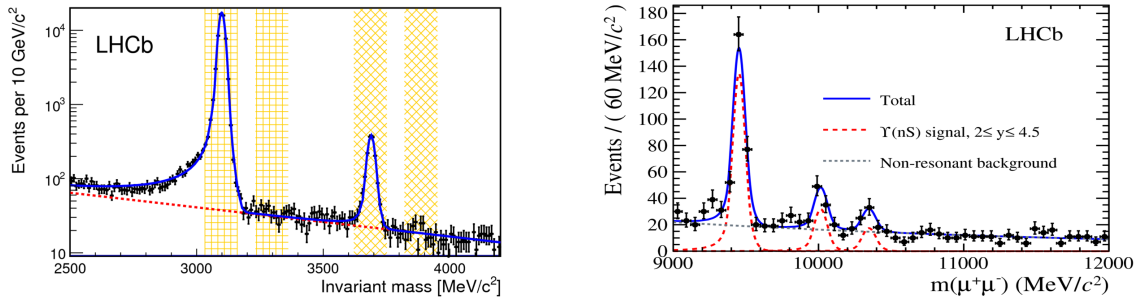

Figure 1: Invariant mass of dimuons in (left) the charmonium analysis [5] with the J/ψ and $\psi(2S)$ signal and sideband windows indicated by the yellow shaded bands and (right) the bottomonium analysis [6].

are consistent with those found at HERA extrapolated to the LHCb kinematic region. In total, $(59.2 \pm 1.2)\%$ of the J/ψ sample and $(52 \pm 7)\%$ of the $\psi(2S)$ sample is estimated to come from exclusive production. The differential cross–sections as a function of meson rapidity y are shown in Fig. 2, compared to LO and approximate Next to Leading Order (NLO) predictions [8]. The

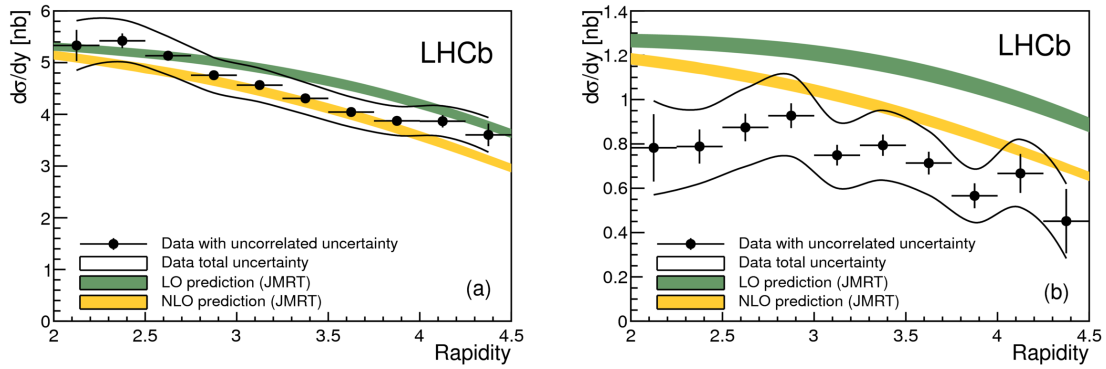

Figure 2: Differential cross-sections for exclusively produced (left) J/ψ and (right) $\psi(2S)$, compared to LO and approximate NLO predictions [8].

integrated cross-sections multiplied by the branching fractions for both muons in the pseudorapidity range $2 < \eta < 4.5$ are in good agreement with theoretical calculations [9–13]. The photoproduction cross–section $\sigma_{\gamma p \to J/\psi(\psi(2S))p}(W)$, as a function of the γp center of mass energy W can be obtained from the differential cross–sections by including rapidity gap correction and photon flux factors, up

to a two–fold ambiguity arising from not knowing which one of the two proton emitted the photon. This can be resolved for one of the solutions using a power–law as derived by H1 at HERA. The corresponding model–dependent cross–section obtained with this method is shown in Fig. 3, where

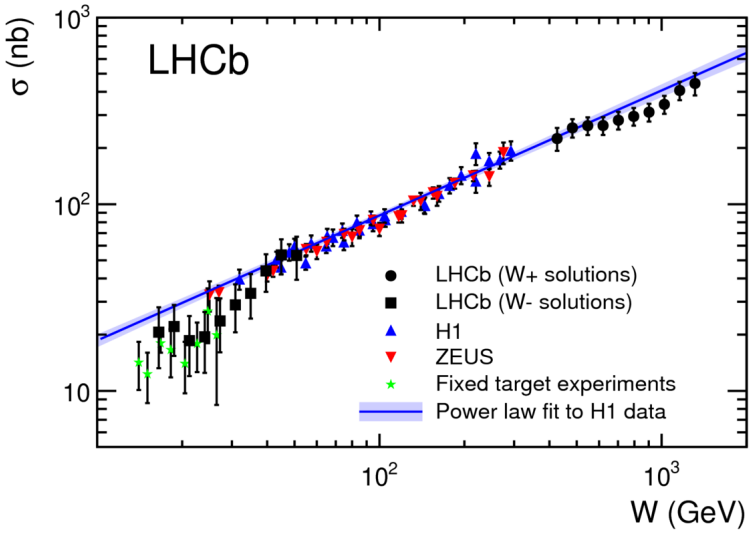

Figure 3: Compilation of photoproduction cross-sections from various experiments [14–18] for J/ψ with the power-law fit from [19] superimposed. The LHCb results are model-dependent as explained in the text.

the two groups of correlated results from LHCb are compared with data points from HERA and fixed–target experiments [14–18]. The results are also in good agreement with the measurements performed in proton-lead collisions at ALICE [20], where the ambiguity mentioned above can be resolved, as the photon, to good approximation, is emitted from the ion. An analysis of J/ψ CEP with data collected at $\sqrt{s} = 13$ TeV has also been carried out [22] including data from the recently installed forward counters. The inclusion of the new counters reduces the inelastic background by about a factor two with repsect to the previous measurements thanks to the extended pseudorapidity veto.

2.2 Photoproduction of $\Upsilon(nS)$ mesons

The selection of Υ meson candidates [6] produced through CEP requires two muons in the LHCb acceptance and no other charged tracks. The muon pair must have $p_T^2 < 2$ GeV^2/c^2 and an invariant mass between 9 and 20 GeV/c^2. The invariant mass distribution of the selected candidates is shown in Fig. 1 (right). Feed-down backgrounds in the $\Upsilon(1S)$ mass window, coming from the various χ_b is estimated in the same way as for the charmonium analysis normalising to selected $\chi_b \to \Upsilon\gamma$ candidates in data. This background is estimated to contribute $(39 \pm 7)\%$ of the total signal yield. As in the charmonium analysis, inelastic $\Upsilon(nS)$ production is estimated by fitting the p_T^2 distribution, but with the signal shape given by the SUPERCHIC generator [23]. After subtraction of the feed–down component, the exclusively produced signal yield is estimated to be $(54 \pm 11)\%$. The differential cross–section for the $\Upsilon(1S)$ state candidates as a function of meson rapidity is shown in Fig. 4.

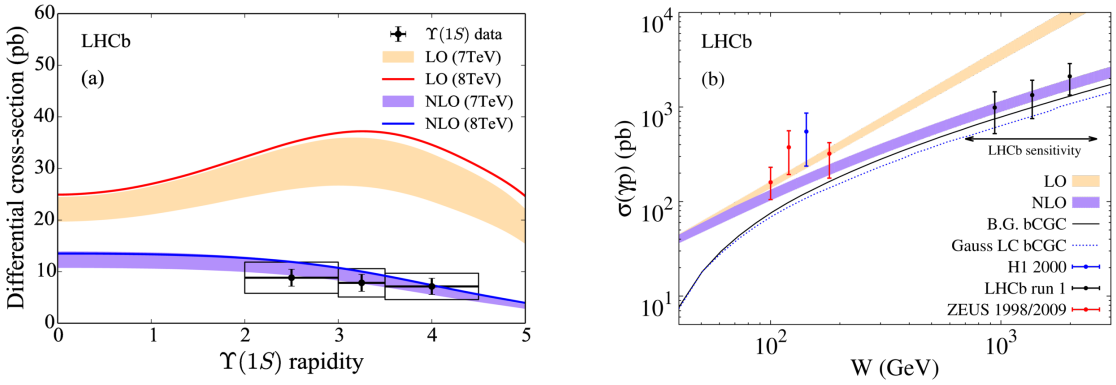

Figure 4: Differential cross-sections (left) and compilation of photoproduction cross-sections from various experiments [24–26] (right) for exclusively produced $\Upsilon(1S)$, compared to LO and NLO predictions [8, 21]. The LHCb results (black dots) are obtained neglecting the smaller of the two ambiguos solutions in the extraction of the photoproduction cross-section, as explained in the text.

The low statistics and high relative background does not allow such measurement for the $\Upsilon(2S)$ and $\Upsilon(3S)$ states. The measured differential cross–section is in very good agreement with the NLO predictions. As for the charmonium analysis, a photoproduction cross–section can be extracted from these results. In the case of Υ states, the smaller of the two ambiguous solutions (that contributes between 5% and 20%) is ignored. The result is shown in Fig. 4 and it is in very good agreement with the NLO calculations and consistent with HERA results [24–26].

3. Multi-parton interactions

Multi–parton interactions occur when two or more independent pairs of partons take part to the scattering process in a single proton-proton collision. These processes represent a potentially important background to physics studies like Higgs boson production or searches for new particles.

3.1 Double charm production involving open charm

At LHC, the large open charm and charmonium production cross–sections [27, 28] make the multi–charm production cross–section relevant. Therefore, a study of multiple charmed particle production represents a valuable tool to study these processes; in addition it sheds light on charmonium production mechanisms [29]. Leading order calculations in perturbative QCD for double open charm and open charm in association with charmonium are available [30–34]. In proton–proton collisions, additional contributions from other mechanisms, such as Double Parton Scattering (DPS) [35–38] or the intrinsic charm content of the proton [35] to the total cross-section, are possible. DPS contributions can be estimated, neglecting partonic correlations in the proton, as the product of the cross-sections of the sub-processes involved divided by an effective cross-section [30–34], via the so–called pocket formula:

$$\sigma^{DPS}_{C_1C_2} = \alpha \frac{\sigma_{C_1} \times \sigma_{C_2}}{\sigma^{DPS}_{eff}}, \tag{3.1}$$

where C_1 and C_2 refer to the two produced charmed particles, α is a parameter which depends on the C_1C_2 combination and σ_{eff}^{DPS} is an effective cross–section related to the transverse overlap function between the partons in the protons.

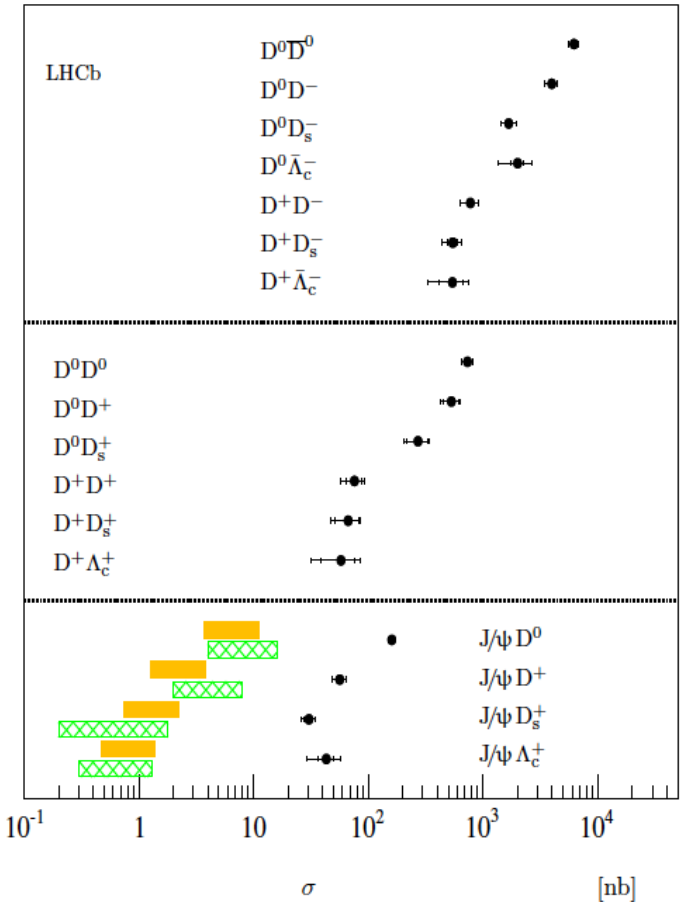

Figure 5: Measured cross-sections [41] $\sigma_{J/\psi C}$, σ_{CC} and $\sigma_{C\bar{C}}$ (points with error bars) compared, in J/ψC channels, to the calculations in [33, 34] (hatched areas) and [40] (shaded areas). The inner error bars indicate the statistical uncertainty whilst the outer error bars indicate the sum of the statistical and systematic uncertainties in quadrature. Charge-conjugate modes are included.

At LHCb, a measurement of open charm (indicated generically as C in the following) in association with J/ψ and double open charm production cross–sections has been performed [41, 42], using 355 pb^{-1} of data taken at $\sqrt{s} = 7$ TeV. The candidate J/ψ mesons were reconstructed from dimuon final states while open charm was reconstructed through the exclusive decays $D^0 \to K^-\pi^+; D^+ \to K^-\pi^+\pi^+; D_s^+ \to K^-K^+\pi^+; \Lambda_c^+ \to pK^-\pi^+$. Signals with a statistical significance in excess of five standard deviations have been observed for four J/ψC modes: $J/\psi D^0$, $J/\psi D^+$, $J/\psi D_s^+$ and $J/\psi\Lambda_c^+$, for six CC modes: D^0D^0, D^0D^+, $D^0D_s^+$, $D^0\Lambda_c^+$, D^+D^+ and $D^+D_s^+$ and for seven C$\bar{\text{C}}$ channels: $D^0\bar{D}^0$, D^0D^-, $D^0D_s^-$, $D^0\bar{\Lambda}_c^-$, D^+D^-, $D^+D_s^-$ and $D^+\bar{\Lambda}_c^-$. The measured cross–sections are summarised in Fig. 5.

The ratios

$$\mathscr{R}_{C_1C_2} \equiv \alpha' \frac{\sigma_{C_1} \times \sigma_{C_2}}{\sigma_{C_1C_2}}, \tag{3.2}$$

where α' is a parameter which depends on the C_1C_2 combination, are shown in Fig. 6.

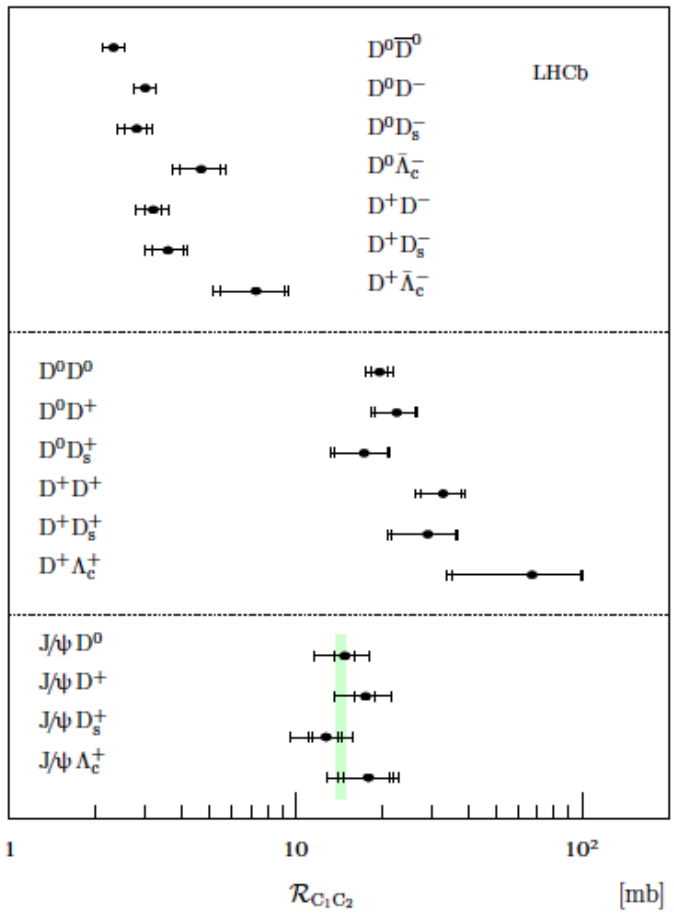

Figure 6: Measured ratios [41] $\mathscr{R}_{C_1C_2}$ (points with error bars) in comparison with the expectations from DPS using the cross-section measured at Tevatron for multi-jet events (light green shaded area). The comparison is made in the DPS approach using the pocket formula. The inner error bars indicate the statistical uncertainty whilst the outer error bars indicate the sum of the statistical and systematic uncertainties in quadrature. For the J/ψC channels the error due to the unknown polarization is also included (outermost error bar)

For the J/ψC and CC cases, in the DPS approach, these ratios can be interpreted as the effective cross–section of eq. (3.1) which should be the same for all modes. The values of the effective DPS cross–section calculated from these modes using the pocket formula are in reasonable agreement with the value measured in multi-jet production at Tevatron $\sigma_{eff}^{DPS} = 14.5 \pm 1.7^{+1.7}_{-2.3}$ mb [43]. For the $C\bar{C}$ modes, the interpretation of the ratios is less direct, but they are expected to be approximately the same for all the final states. These measurements suggest that DPS is the dominant process for the above modes. This is also supported by the analysis of kinematical variables where correlation effects are expected in single parton scattering, e.g. the difference in azimuthal angle $\Delta\varphi$ and in rapidity Δy between the two charmed particles. The distribution of all the variables

studied for the double–charm final states considered are compatible with the absence of correlation indicating again the dominance of DPS.

3.2 Production of associated Υ and open charm hadrons

The associated production of bottomonium and open charm hadrons has also been studied at LHCb using an integrated luminosity of 3 fb^{-1} collected at $\sqrt{s} = 7$ and 8 TeV [44]. The Υ candidates are reconstructed in their dimuon final state while the charmed hadrons are reconstructed as described in the previous section. Five combinations, $\Upsilon(1S)D^0$, $\Upsilon(2S)D^0$, $\Upsilon(1S)D^+$, $\Upsilon(2S)D^+$ and $\Upsilon(1S)D_s^+$ are observed with statistical significance larger than 5σ. The invariant mass distributions for the ΥD^0 candidates is shown in Fig. 7.

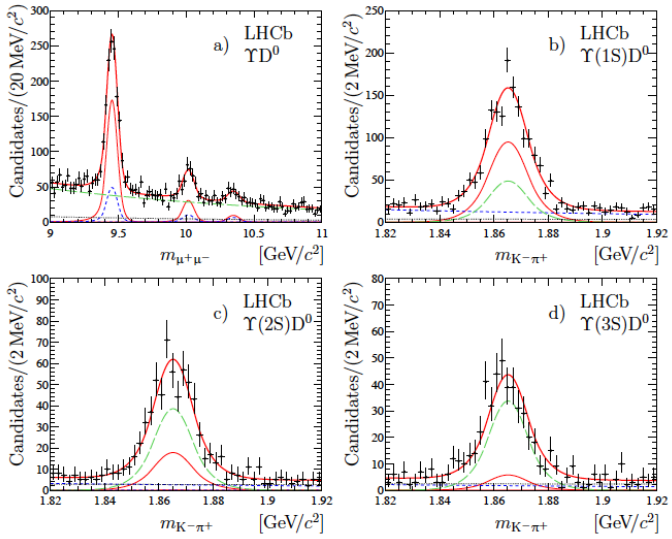

Figure 7: Invariant mass distributions for the selected candidates $\Upsilon(nS)$ and D^0 in associated production. The curves are the projections of a two–dimensional maximum likelihood fit as described in [44].

Production cross-sections are measured for $\Upsilon(1S)D^0$ and $\Upsilon(1S)D^+$. The derived σ_{eff}^{DPS}, eq. (3.1), is consistent with the result from Tevatron [43]. The measured cross-sections and the differential distributions indicate the dominance of double parton scattering as the main production mechanism.

4. Conclusion

A wide physics program on QCD is being pursued by LHCb, which exploits its unique geometry to complement other LHC experiments. In these proceedings selected results on central exclusive production and double charm and bottom–charm associated production have been presented showing the physics potential of LHCb in the QCD domain. The CEP measurements provide useful information in understanding the proton structure while the double final state measurements shed additional light on double parton scattering. Many other results have been released by LHCb using data collected at $\sqrt{s} = 7$ TeV and 8 TeV. Many other results are also expected with data at $\sqrt{s} = 13$ TeV.

References

[1] Alves A. A. Jr *et al.* (LHCb collaboration), *JINST* **3** (2008) S08005.

[2] M. Albrow *et al.* (FSC Team and CMS and HERSCHEL Team and LHCb collaborations), *Int. J. Mod. Phys. A* **29** (2014) no.28, 1446018.

[3] M.G. Albrow, T.D. Coughlin, J.R. Forshaw, *Prog. Part. Nucl. Phys.* **65** (2010) 149.

[4] M.G. Albrow, *Int. J. Mod. Phys. A* **29** (2014) 1402006.

[5] R. Aaij *et al.* (LHCb collaboration), *J. Phys. G* **41** (2014) 055002, [arXiv:1401.3288].

[6] R. Aaij *et al.* (LHCb collaboration), *JHEP* **1509** (2015) 084, [arXiv:1505.08139].

[7] R. Aaij *et al.* (LHCb collaboration), *J. Phys. G* **41** (2014) 115002 [arXiv:1407.5973].

[8] S.P. Jones *et al.*, *JHEP* **11** (2013) 085, [arXiv:1307.7099];
S.P. Jones *et al.*, *J. Phys. G* **41** (2014) 055009, [arXiv:1312.6795].

[9] V.P. Gonçalves, M.V.T. Machado, *Phys. Rev. C* **84** (2011) 011902, [arXiv:1106.3036].

[10] L. Motyka, G. Watt,*Phys. Rev. D* **78** (2008) 014023, [arXiv:0805.2113].

[11] W. Schafer, A. Szczurek, *Phys. Rev. D* **76** (2007) 094014, [arXiv:0705.2887].

[12] S.R. Klein, J. Nystrand, *Phys. Rev. Lett.* **92** (2004) 142003, [hep-ph/0311164].

[13] L.A. Harland-Lang *et al.*, *Eur. Phys. J. C* **76** (2016) 9, [arXiv:1508.02718].

[14] A. Aktas *et al.* (H1 Collaboration), *Eur. Phys. J. C* **46** (2006) 585, [arXiv:hep-ex/0510016].

[15] S. Chekanov *et al.* (ZEUS Collaboration), *Eur. Phys. J. C* **24** (2002) 345, [arXiv:hep-ex/0201043].

[16] M. E. Binkley *et al.*, *Phys. Rev. Lett.* **48** (1982) 73.

[17] B. H. Denby *et al.*, *Phys. Rev. Lett.* **52** (1984) 795.

[18] P. L. Frabetti *et al.* (E687 collaboration), *Phys. Lett. B* **316** (1993) 197.

[19] C. Alexa *et al.* (H1 collaboration), *Eur. Phys. J. C* **73** (2013) 2466.

[20] B. Abelev *et al.* (ALICE collaboration), *Phys. Rev. Lett.* **113** (2014) 232504, [arXiv:1406.7819].

[21] V. P. Gonçalves, B. D. Moreira and F. S. Navarra, *Phys. Lett. B* **742** (2015) 172, [arXiv:1408.1344 [hep-ph]].

[22] LHCb collaboration, *LHCb-CONF-2016-007* (2016).

[23] L.A. Harland-Lang *et al.*, *Eur. Phys. J. C* **76** (2016) 9, [arXiv:1508.02718].

[24] J. Breitweg et al. (ZEUS collaboration), *Phys. Lett. B* 437 (1998) 432, [hep-ex/9807020].

[25] C. Adloff *et al.* (H1 collaboration), *Phys. Lett. B* **483** (2000) 23, [hep-ex/0003020].

[26] S. Chekanov *et al.* (ZEUS collaboration), *Phys. Lett. B* **680** (2009) 4, [arXiv:0903.4205].

[27] [1] LHCb collaboration, *LHCb-CONF-2010-013* (2010).

[28] R. Aaij *et al.* (LHCb collaboration), *Eur. Phys. J. C* **71** (2011) 1645, [arXiv:1103.0423].

[29] S.J. Brodsky and J.-P. Lansberg, *Phys. Rev. D* **81** (2010) 051502, [arXiv:0908.0754].

[30] V. Kartvelishvili and S. Esakiya, (in Russian), *Yad. Fiz.* **38** (1983) 722.

[31] B. Humpert and P. Mery, *Z. Phys. C* **20** (1983) 83.

[32] A. Berezhnoy, A. Likhoded, A. Luchinsky and A. Novoselov, *Phys. Rev. D* **84** (2011) 094023 [arXiv:1101.5881].

[33] A. Berezhnoy, V. Kiselev, A. Likhoded and A. Onishchenko, *Phys. Rev. D* **57** (1998) 4385, [hep-ph/9710339].

[34] S. Baranov, *Phys. Rev. D* **73** (2006) 074021.

[35] C. Kom, A. Kulesza and W. Stirling, *Phys. Rev. Lett.* **107** (2011) 082002, [arXiv:1105.4186].

[36] S. Baranov, A. Snigirev and N. Zotov, *Phys. Lett. B* **705** (2011) 116, [arXiv:1105.6276].

[37] A. Novoselov, [arXiv:1106.2184].

[38] M. Luszczak, R. Maciula and A. Szczurek, [arXiv:1111.3255].

[39] S. Brodsky, P. Hoyer, C. Peterson and N. Sakai, *Phys. Lett. B* **93** (1980) 451.

[40] J. Lansberg, *Eur. Phys. J. C* **61** (2009) 693, [arXiv:0811.4005].

[41] R. Aaji *et al.* (LHCb collaboration), *JHEP* **06** (2012) 141.

[42] R. Aaji *et al.* (LHCb collaboration), *JHEP* **03** (2014) 108.

[43] F. Abe *et al.* (CDF collaboration), *Phys. Rev. D* **56** (1997) 3811.

[44] R. Aaij *et al.* (LHCb Collaboration), *JHEP* **07** (2016) 052, [arXiv:1510.05949].